KLA INSTRUMENTS

Measuring Storage and Loss Modulus of Artificial Tissue

Nano Indenter® G200

Introduction

Real biological tissue is perishable and expensive, especially if the origin is human. Therefore, researchers prefer to develop techniques for imaging, testing, cutting, and so forth on less valuable, inorganic materials. Researchers at the University of Wisconsin have developed such materials, called "phantoms", for evaluating and improving magnetic-resonance and ultrasound imaging systems[1-4]. In order to function as a substitute, these materials had to be temporally stable and mechanically comparable to real tissue. In this work, we developed a technique for measuring the storage and loss modulus of such materials using dynamic indentation[5,6] on a KLA Nano Indenter® G200.

Samples

Samples for this work, shown in Figure 1, were provided by researchers at the University of Wisconsin. The materials were dispersions of vegetable oil in gelatin. Previous work had revealed that mechanical properties could be controlled by controlling the volume fraction of oil in the dispersion – higher oil content produced more a compliant material. Details of production are provided elsewhere[1-4]. Samples were stored and tested in a bath of vegetable oil, as shown in Figure 2, to prevent desiccation. Results from two samples are reported here. The first, sample S, was relatively stiff, having a storage modulus on the order of MPa; the second, sample C, was very compliant, having a storage modulus on the order of kPa.

Instrumentation and Test Method

Tests were performed on a G200 using the CSM option, which allows frequency-specific testing. Both samples were tested with a flat-ended cylindrical punch. For sample S, a 1mm (diameter) punch was used; for sample C, a 2mm punch was used. We chose the flat-punch geometry in order to have a known contact area, independent of penetration depth.

On the Nano Indenter G200, the vertical position of the sample is fixed during testing; adjustment of sample height is unnecessary because the G200 has a travel range of 1.5mm. The entire travel range can be used during a single test, or the range can be reduced to a smaller span near the surface position in order to increase resolution. This flexibility offers a definite advantage when testing polymers, because sample compliance and the need to bring the punch face into full contact often necessitate a larger travel range than is typically used for indentation testing on harder materials.

Figure 1. "Phantom" tissue supplied by researchers at the University of Wisconsin.

Figure 2. Phantom tissue as mounted for testing in fluid.

A single test consists of the following segments, in order:

1. The sample moves into position under the indenter.
2. The indenter senses and records the vertical position of the test surface.
3. The sample moves out from under the indenter.
4. With the sample out of the way, the indenter returns to the position, within the 1.5mm travel range, at which it sensed the surface.
5. The dynamic response of the instrument is measured for each frequency at which the test material will be evaluated.
6. The indenter is raised up (out of the way).
7. The sample moves back into position under the indenter.
8. The indenter moves into full contact with the sample surface.
9. The dynamic response of the system (where "system" means the combination of the instrument together with the contact) is evaluated as a function of frequency.

The value of steps 4 and 5 in the above procedure may not be immediately obvious; because these materials are so compliant, the influence of the contact on the system dynamic response is subtle. Therefore, the influence of the instrument on the system dynamic response must be very well known in order to accurately deduce the dynamic response of the contact. Since the dynamic response of the instrument is a function of both indenter position (within its 1.5mm range of travel) and oscillation frequency, steps 4 and 5 accomplish the task of measuring the response of the instrument at the vertical position for the test and at each test frequency.

Analysis

The indentation head on the Nano Indenter G200 is illustrated schematically in Figure 3. When the indenter is not in contact with the sample, this mechanism is modeled by the simple harmonic oscillator shown in Figure 4; here, K_s is the stiffness of the supporting leaf springs, m is the mass, and D is the damping. Standard analysis of any such simple-harmonic oscillator reveals that the dynamic stiffness of the instrument is given by:

$$K_s - m\omega^2 = (F_0/z_0) \cdot \cos\varphi \,|_{\text{instrument}} \qquad (1)$$

where ω is the angular forcing frequency, F_0 is the amplitude of the force oscillation, z_0 is the amplitude of the (resulting) displacement oscillation, and φ is the phase angle by which the force oscillation leads the displacement oscillation. Likewise, the dynamic damping of the instrument is given by:

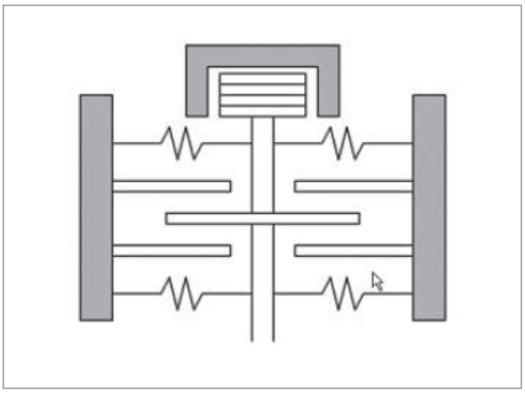

Figure 3. Schematic of freehanging indenter.

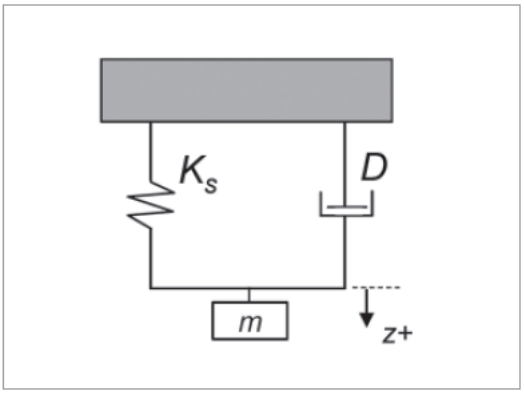

Figure 4. Dynamic model of instrument alone (no contact).

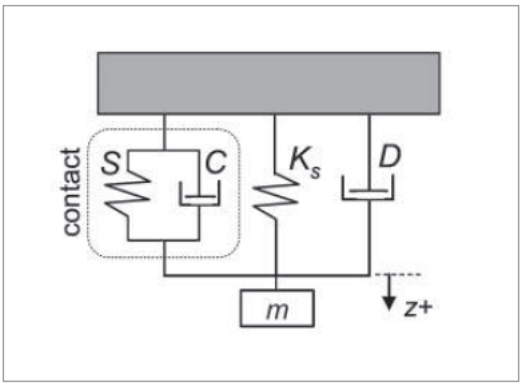

Figure 5. The distinct hardness curves for the two different phases of the material.

$$D\omega = (F_0/z_0) \cdot \sin\varphi \,|_{\text{instrument}} \qquad (2)$$

Once the indenter is in full contact with the sample, the indentation head and contact are modeled together, as shown in Figure 5 (for explanation purposes, we have neglected the influence of the stiffness of the load frame, but it is included in the actual analysis in the KLA G200 software). Because two springs in parallel can be treated as one by adding their

stiffnesses, the dynamic stiffness for the system in Figure 5 is given by:

$$(K_s + S) - m\omega^2 = (F_0/z_0) \cdot \cos\varphi \,|_{system} \quad (3)$$

Likewise, the dynamic damping of the system is given by:

$$(C + D)\omega = (F_0/z_0) \cdot \sin\varphi \,|_{system} \quad (4)$$

Therefore, in order to get the contact stiffness, S, we subtract Equation (1) from Equation (3) and simplify:

$$S = (F_0/z_0) \cdot \cos\varphi \,|_{system} - (F_0/z_0) \cdot \cos\varphi \,|_{instrument} \quad (5)$$

Likewise, in order to get the contact damping, $C\omega$, we subtract Equation (2) from Equation (4) and simplify:

$$C\omega = (F_0/z_0) \cdot \sin\varphi \,|_{system} - (F_0/z_0) \cdot \sin\varphi \,|_{instrument} \quad (6)$$

Equation (5) and Equation (6) reveal that when the instrument makes a substantial contribution to the system dynamic response, as is the case when testing very compliant materials, accurate assessment of the instrument contribution is essential. This relation is why we evaluate the instrument contribution at the same frequencies, with the indenter in exactly the same position, as is used for the actual test.

Once the contact stiffness and damping are known from Equation (5) and Equation (6), values for the storage modulus (E'), loss modulus (E''), and loss factor $tan\delta$ are calculated as:

$$E' = (\sqrt{\pi}/2) \cdot (S/\sqrt{A}) \quad (7)$$

$$E'' = (\sqrt{\pi}/2) \cdot (C\omega/\sqrt{A}) \quad (8)$$

$$tan\delta = E''/E' = C\omega/S \quad (9)$$

where A is the contact area of the punch face. The loss factor, $tan\delta$, is an experimentally advantageous parameter for ultra-compliant materials because the contact area does not come into its calculation, and thus, need not be known.

Results

The results for storage modulus and loss modulus as a function of frequency for sample S (the relatively stiff sample) are shown in Figure 6. Figure 7 shows the storage modulus for sample C (the relatively compliant sample). Even though sample C was tested with a 2mm punch, the contact did not produce damping that was significantly different from the instrument alone, and so loss modulus could not be determined for sample C. A larger diameter indenter could solve this problem at the sacrifice of spatial resolution.

Discussion

The results presented here are in good agreement with results obtained on bulk samples using dynamic mechanical analysis

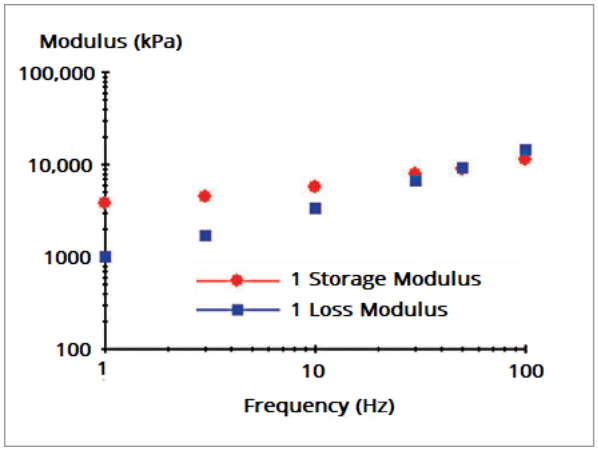

Figure 6. Storage and loss modulus as a function of frequency for phantom tissue sample S.

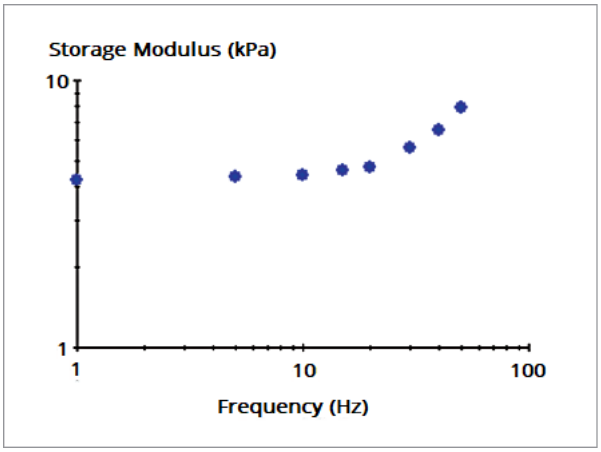

Figure 7. Storage modulus as a function of frequency for phantom tissue sample C.

(DMA). However, dynamic indentation offers the advantage of better spatial resolution in determining mechanical properties. The materials tested here are intended to be used to create test samples for magnetic-resonance and ultrasound imaging systems. The test samples created for imaging systems must have spatial variations in mechanical properties similar to those that occur in real tissue in the vicinity of tumors, cysts, etc.

Therefore, the Nano Indenter G200 is a useful tool in this context for at least two reasons: first, it can be used to measure properties of actual tissue in order to be able to create artificial tissue with similar variations in mechanical properties; second, it can be used to measure the properties of the artificial tissue to verify similarity to real tissue and to provide a reference for analogous information from the imaging system.

The techniques presented in this work will likely find other applications in biomaterials. For example, when culturing cells, the modulus of the gel substrate on which the cells are grown strongly affects the form and function of the resulting cells[7]. Therefore, a means for quantitatively measuring gel modulus will aid the development of techniques for in vitro tissue growth.

Technology and Applications

The Nano Indenter G200 is powered by electromagnetic actuation to achieve unparalleled dynamic range in force and displacement. The instrument's unique design avoids lateral displacement artifacts, while software compensates fully for any drift in force. Using the G200, researchers can measure Young's modulus and hardness in compliance with ISO 14577. Deformation can be measured over six orders of magnitude (from nanometers to millimeters).

With the CSM option, the KLA Nano Indenter applies a load to the indenter tip to force the tip into the surface while simultaneously superimposing an oscillating force with an amplitude generally several orders of magnitude smaller than the nominal load. The CSM option offers a means of separating the in-phase and out-of-phase components of the load-displacement history. This separation provides an accurate measurement of the location of initial surface contact and continuous measurement of contact stiffness as a function of depth or frequency, thus eliminating the need for unloading cycles. Since the contact stiffness is determined directly, no assumptions (such as mechanical equilibrium) are required to correct for elasticity.

Applications of the G200 include semiconductor, thin films and MEMs (wafer applications); hard coatings and DLC films; composite materials, fibers and polymers; metals and ceramics, and biomaterials and biology.

References

1. E.L. Madsen, G.R. Frank, T.A. Krouskop et al. "Tissue-mimicking oil-in-gelatin dispersions for use in heterogeneous phantoms," Ultrasound Imaging, vol. 25, pp.17-38, 2003.
2. E.L. Madsen, M.A. Hobson, H. Shi, T. Vargese and G.R. Frank, "Stability of heterogeneous elastography phantoms made from oil dispersions in aqueous gels," Ultrasound in Medicine and Biology, vol. 32, No. 2, pp. 261-270, 2006.
3. E.L. Madsen, G.R. Frank, H. Shi, J. Jiang, T.J. Hall, T. Vargese, M.M. Doyley and J.B. Weaver, "Anthropomorphic breast phantoms for testing elastography systems," Ultrasound in Medicine and Biology, vol. 32, No. 6, pp. 857-874, 2006.
4. E.L. Madsen, G.R. Frank, M.A. Hobson, H. Shi, J. Jiang, T. Vargese and T.J. Hall, "Spherical lesion phantoms for testing the performance of elastography systems," Journal of Materials Research, Vol. 50, pp. 5983- 5995, 2005.
5. W.C. Oliver and G.M. Pharr, "An improved technique for determining hardness and elastic modulus using load and displacement sensing indentation experiments," Journal of Materials Research, vol. 7(6), pp. 1564-1583, June 1992.
6. J.L. Loubet, B.N. Lucas and W.C. Oliver, "Some measurements of viscoelastic properties with the help of nanoindentation," NIST Special Publication 896: International Workshop on Instrumented Indentation, pp. 31-34, 1995.
7. E.J. Semler, C.S. Ranucci and P.V. Moghe, "Mechanical manipulation of hepatocyte aggregation can selectively induce or repress liver-specific function," Biotechnology and Bioengineering Vol. 69(4), pp. 359-369, August 20, 2000.

KLA Corporation
One Technology Drive
Milpitas, CA 95035
Printed in the USA
Rev 3 2020-10-05